J Math Chem (2012) 50:2577–2605
DOI 10.1007/s10910-012-0048-0

ORIGINAL PAPER

Direct and closed form analytical model for the prediction of reaction kinetic of EPDM accelerated sulphur vulcanization

G. Milani · F. Milani

Received: 25 May 2012 / Accepted: 5 July 2012 / Published online: 24 July 2012

Abstract A novel direct model with kinetic base for the prediction of the final vulcanization level of EPDM cured with sulphur is presented. The model bases on a preliminary characterization of rubber through standard rheometer tests and allows an accurate prediction of the crosslinking degree at both successive curing times and different controlled temperatures. Both the case of indefinite increase of the torque and reversion can be handled. The approach proposed bases on a previously presented exponential model, where a calibration of three kinetic constants at fixed temperature by means of non-linear least square fitting was required. Here the exponential model is superseded and kinetic constants are evaluated through simple closed form formulas. The applicability of the approach is immediate and makes the model extremely appealing when fast and reliable estimates of crosslinking density of cured EPDM are required. To show the capabilities of the approach proposed, a comprehensive comparison with both available experimental data and results obtained numerically with the exponential model for real compounds at different temperatures is finally provided.

Keywords Simplified kinetic model · Closed form solution · Sulphur vulcanization · Reversion · Rheometer curve fitting

G. Milani (✉)
Politecnico di Milano, Piazza Leonardo da Vinci 32, 20133 Milan, Italy
e-mail: milani@stru.polimi.it; gabriele.milani@polimi.it

F. Milani
CHEM.CO Consultant, Via J.F. Kennedy 2, 45030 Occhiobello, Rovigo, Italy
e-mail: federico-milani@libero.it

1 Introduction

In order to guarantee a good level of vulcanization, macroscopically intended as good mechanical performance of the items after curing, the level of reticulation reached point by point by a rubber specimen subjected to prescribed temperature and cure time conditions should be predicted by means of reliable theoretical or numerical models.

As a matter of fact, the most diffused system of vulcanization is represented by accelerated sulphur curing. While the utilization of peroxides to vulcanize rubber would be preferable, being the links determined by transversal chains largely more stable (energy 346 KJ/mole against 272 KJ/mole [1]), sulphur is normally preferred merely for economic reasons.

Unfortunately, unlike peroxidic curing, sulphur vulcanization chemistry is rather intricate, since crosslink is associated to complex reactions occurring in series and parallel. For this reason, to propose a quantitative macroscopic model able to predict vulcanization in terms of rubber physical properties is still a true challenge. At present, it can be stated that, while the utilization of sulphur is quantitatively predominant, its chemistry of vulcanization remains an open issue, despite its discovery and utilization go back to Goodyear [2–7].

To be fully predictive, a numerical model should take into account the distinctive aspects of sulphur vulcanization, being reversion the most important. Reversion occurs quite frequently in practice and consists in a remarkable decrease of rubber vulcanized properties at the end of the curing process. Chen et al. [8] have shown that this phenomenon seems to appear when two reactions are competing during vulcanization. Reversion is often associated with high-temperature curing. In agreement with the studies conducted by Loo [9], it can be stated that, generally, when the cure temperature rises, the crosslink density drops, thus increasing the degree of reversion. Morrison and Porter [10] confirmed that the observed reduction in vulcanizate properties is caused by two reactions proceeding in parallel, i.e. de-sulphuration and decomposition, see Fig. 1.

The commonly accepted experimental test at the base of any numerical/analytical model for sulphur curing is the so-called rheometer test [11,12]. The fundamental importance of this test for the experimental characterization of crosslinking has been acknowledged in the recent past by many authors, especially Poh and co-workers [13–18].

Such standard test is usually performed maintaining a small rubber cylindrical specimen inside a chamber at fixed vulcanization temperature, where a metallic disc oscillates. Torque resistance to oscillation is registered at increasing exposition times and plotted in a so-called rheometer chart or cure curve thus giving indirect macroscopic information on rubber reticulation kinetics at fixed temperature. Nowadays, different rheometers are at disposal in the market, ranging from traditional devices equipped with metallic oscillating discs (ODR) to rotor-less [19,20] (RPA2000) instruments, where the oscillating part is removed to reduce spourious secondary torques induced by inertia and friction. In any case, all devices are able to register the torque variation (or rotation resistance) during the test. Typically, both natural and synthetic rubber exhibit a decrease in the initial part of the test, followed by a sudden increase at

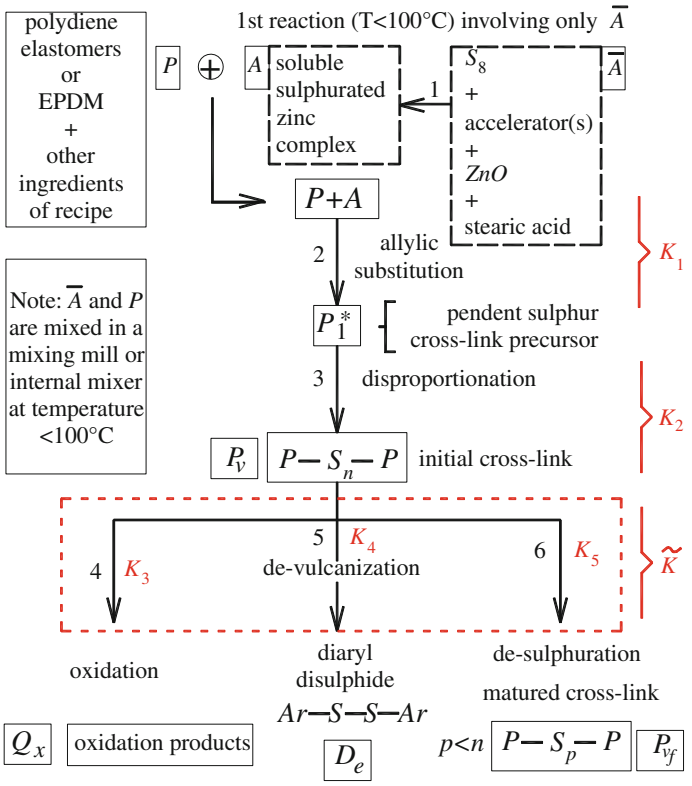

Fig. 1 Products and schematic reaction mechanisms of accelerated sulphur vulcanization of poly-diene and EPDM elastomers

approximately 1/3 of time needed to complete the test (scorch time). In several cases, torque decreases near the end of the experimentation. Such behavior is commonly associated to reversion. A single compound has its own characteristic cure curve at fixed temperature, which characterizes macroscopically the reticulation of the compound. A change in both accelerators molar ratios and temperature room changes the cure curve.

Basing almost exclusively on experimental rheometer charts, pioneering analytical contributions in the right direction are due to some authors, who proposed simplified approaches for the practical evaluation of the final crosslinking degree of vulcanized items. Among the others, [21–26] models may be acknowledged. Conceived essentially for natural rubber, they basically rely into simplified kinetic models enforced to follow differential equations similar to those used for peroxidic curing, basing on an experimental data fitting to deduce kinetic constants.

To circumvent limitations of such models in the application of EPDM rubber, the mechanisms at the base of vulcanization for such blend should be properly considered. In this framework, focusing exclusively on EPDM rubber, the commonly accepted basic reactions involved–see also [27–30], Fig. 1, may be regarded to be the following:

$$
\begin{aligned}
&(a)\quad P + A \overset{K_1}{\rightarrow} P_1^* \\
&(b)\quad P_1^* \overset{K_2}{\rightarrow} P_v \\
&(c)\quad P_v \overset{K_3}{\rightarrow} Q_x \\
&(d)\quad P_v \overset{K_4}{\rightarrow} D_e \\
&(e)\quad P_v \overset{K_5}{\rightarrow} P_{v_f}
\end{aligned}
\tag{1}
$$

In Eq. (1), P and A are the polymer (EPDM) and soluble sulphureted zinc complex (S_8 + accelerators + ZnO + stearic acid) respectively, P_1^* is the pendent sulfur (cross-link precursor), P_v is the reticulated EPDM, P_{v_f} is the matured cross-link, Q_x is the oxidation product, D_e represents diaryl-disulphide and $K_{1,\ldots,5}$ are kinetic reaction constants. Here it is worth emphasizing that $K_{1,\ldots,5}$ are temperature dependent quantities, hence they rigorously should be indicated as $K_{1,\ldots,5}(T)$, where T is the absolute temperature. In what follows, for the sake of simplicity, the temperature dependence will be left out.

Reaction (a) in (1) represents the allylic substitution in Fig. 1, reaction (b) is the disproportionation, whereas reactions (c) (d) and (e) occurring in parallel are respectively the oxidation, the de-sulphuration and the de-vulcanization.

A macroscopic interpretation of sulphur vulcanization, which resigns to take its steps on kinetic considerations but bases exclusively on experimental rheometer chart data fitting, has been recently proposed by the authors in [31] and [32], respectively in absence and presence of reversion. The models are merely phenomenological, approximating the rheometer chart by means of two parabolas and one hyperbola. In case of reversion, the hyperbola is rotated with respect to coordinate axes. While the application of such model is very straightforward for practical purposes, the absence of a kinetic base does not permit to generalize the models to any vulcanization temperature directly from the numerical model and a huge amount of experimental data is needed.

To supersede such limitation, very recently, Milani and Milani [33,34] have presented a relatively simple numerical model basing on actual reaction kinetics (1), where rubber crosslinking density during vulcanization may be found solving a non-homogeneous second order differential equation with unknown constant coefficients. The approach is fully based on reaction kinetic characterizing EPDM sulphur curing. Independent unknown coefficients are only three, and may be regarded as a combination of kinetic constants associated to partial reactions occurring during vulcanization, see also Fig. 1. Milani and Milani [33,34] proposed to estimate numerically independent coefficients through a data fitting on experimental rheometer curves available for a given compound, thus indirectly evaluating the crosslinking degree from a macroscopic test. The approach is mathematically rather simple, but has the drawback of requiring a material identification through non-linear least square routines or genetic algorithms.

Available codes are usually stable, but sometimes may be tedious in the calibration of optimization options, as for instance the choice of the initial iteration values for the independent variables to identify. To circumvent this important limitation of the procedure, and to make it immediately applicable by manufacturers, in the present paper a new approach, which still bases on the original model proposed in [33,34], but allows a kinetic parameters characterization by means of closed form formulas is proposed.

The major improvement relies into the approximation of the cure curve numerically determined through [33,34] models into a modified rheometer chart, where the horizontal axis is replaced by the normalized logarithm of the curing time, by means of three straight lines.

Such approximation allows a direct evaluation, by means of simplified but effective formulas, of the parameters entering the second order differential equation model proposed in [33,34].

The improved model is tested on two different EPDM compounds, both exhibiting some reversion at high temperatures. Rheometer charts so evaluated are compared with curves provided by the model proposed in [33,34], available experimental data and a simplified approached without reversion. Finally kinetic constants so obtained are again compared with those provided by an approach based on linear least square fitting of the second order non homogeneous differential equation by Milani and Milani [33,34].

In both cases considered, results are in excellent agreement with existing literature, exhibiting errors in constants estimations non exceeding 5 %, meaning that the direct procedure presented may be represent a valuable tool for all manufactures interested in a fast prediction of the level of crosslinking of EPDM cured with sulphur, at fixed vulcanization temperature and time conditions.

2 The improved kinetic numerical model

The model hereafter presented takes its steps from the theoretical results obtained in [33,34], superseding the major limitation of such approach, i.e. the tedious non-linear least square numerical evaluation of the kinetic constants at the base of the model.

As well known, non-linear least square routines are not always at disposal to manufacturers, require time to be managed with awareness and sometimes fail to find a solution, especially when a wrong starting point is selected. In addition, the overall procedure may be tedious and in some cases could provide results affected by a certain level of scatter, due to the numerical instabilities related to the number of points sampled to perform the best fitting.

Such major drawback is completely overcome in this paper, as it is shown in detail in this section. To make the model fully clear, the main features related to the exponential model proposed in [33,34] are hereafter briefly recalled.

The worldwide recognized standard experimental test to evaluate macroscopically the vulcanization characteristics of vulcanizable rubber compounds is the so-called oscillating disc or rotorless curometer test [20].

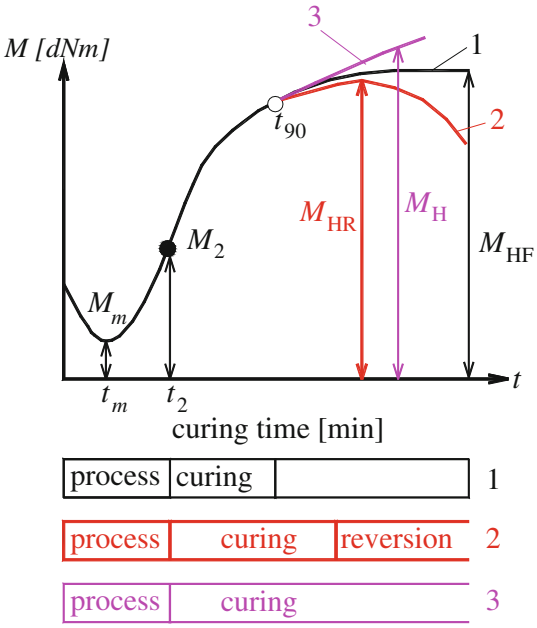

Fig. 2 Typical experimental behaviour of a rubber compound during rheometer test

In one version of such a device (oscillating disc rheometer) the sample of rubber is enclosed within a heated chamber. Vulcanization is measured by the increase in the torque required to maintain a given amplitude of oscillation at a given temperature. The torque is thus roughly proportional to reticulation. The torque is plotted against time to give a so-called rheometer chart, rheograph or cure curve, which exhibits a number of features used to compare cure.

In a rheometer chart, the resistance to oscillation (torque) is measured and recorded as a function of time, as in Fig. 2. In practice, three different cases can occur, as shown in Figs. 2: (1) the curve reaches a maximum asymptotically, (2) the curve reaches a maximum and then decreases (reversion) and (3) the curve increases monotonically after the scorch point t_2. In Fig. 2 the so called t_{90} point is also represented. It is defined as the time to achieve 90 % cure and, mathematically, it is the time for the torque to increase to $90/100(M_{HF} - M_m) + M_m$. t_{90} makes sense only for scorch curves reaching a maximum torque. The second case is encountered very frequently in practice, because reversion is a distinguishing characteristic of sulphur curing (Fig. 1), especially at high temperatures.

The numerical algorithm proposed is based on the experimental use of rheometers following the ASTM D 2084 method [19] at different temperatures to collect a suitable database of experimental data regarding cure curves at increasing temperatures and their successive interpolation by means of a simple kinetic mathematical formulation.

At present, the knowledge regarding the chemistry of accelerated sulphur vulcanization seems a bit fragmented; some useful experimental data are available from Poh et al. [13–18], who observed a marked relation among scorch time, amount of activators used and rheometer temperatures. Unfortunately, numerical and/or theoretical

models in this fields are a few. In this context, an attempt to propose a computer aided procedure to maintain and guarantee a uniform product quality was presented recently in [35], but for PBR and focusing exclusively on Mooney viscosity.

In any case, data reported in the literature are insufficient to fully calibrate the numerical model here proposed. In fact, in order to predict the vulcanization rate during an industrial process of production of thick items, it is necessary to have at disposal from laboratory experimentation, several rheometer curves at different controlled curing temperature inside the rheometer.

Chemical reactions occurring during sulfur vulcanization reported in (1) obey the following rate equations:

$$\begin{aligned}
\frac{dP}{dt} &= -K_1 A P \\
\frac{dP_v}{dt} &= K_2 P_1^* - K_3 Q_x - K_4 D_e - K_5 P_{v_f} \\
\frac{dQ_x}{dt} &= K_3 P_v \\
\frac{dD_e}{dt} &= K_4 P_v \\
\frac{dP_{v_f}}{dt} &= K_5 P_v
\end{aligned} \tag{2}$$

By means of the so called xyz method, independent variables may be established.

From stoichiometry of the reaction, it can be argued that:

$$\begin{aligned}
A &= A_0 - x \\
P &= P_0 - x \\
P_1^* &= x - y = (P_0 - P) - y = (P_0 - P) - \left(P_v + Q_x + D_e + P_{v_f}\right) \\
P_v &= y - z - q - r \\
Q_x &= z \\
D_e &= q \\
P_{v_f} &= r
\end{aligned} \tag{3}$$

where $x = P(t)$, $y = P_v(t)$, $z = Q_x(t)$, $q = D_e(t)$, $r = P_{v_f}(t)$ identify independent variables, P_0 and A_0 are the initial molar concentrations of polymer and curing agent, or better the soluble sulphur agent zinc complex (S_8 + Accelerators + ZnO + Stearic acid) respectively. Typically they are known production parameters (they may obviously vary from case to case) and they are obtained mixing all the components in an internal mixed before vulcanization.

The aim of the approach is to provide an analytical expression for vulcanized rubber, i.e. concentration of $P_v(t)$ with respect to time.

From (2) and (3), the following set of differential equations is deduced:

$$
\begin{aligned}
(a)\quad & \frac{dP}{dt} = -K_1 AP \\
(b)\quad & \frac{dP_v}{dt} = K_2 P_1^* - K_3 Q_x - K_4 D_e - K_5 P_{v_f} \\
& = K_2 \left[(P_0 - P) - \left(P_v + Q_x + D_e + P_{v_f} \right) \right] \\
& \quad -K_3 Q_x - K_4 D_e - K_5 P_{v_f} \qquad (4) \\
(c)\quad & \frac{dQ_x}{dt} = K_3 P_v \\
(d)\quad & \frac{dD_e}{dt} = K_4 P_v \\
(e)\quad & \frac{dP_{v_f}}{dt} = K_5 P_v
\end{aligned}
$$

Obviously the first order differential equation system (4) can be solved using a standard Runge-Kutta numerical approach [36,37]. However, such a procedure, when coupled with a non-linear least square algorithm (as in the present case) may become very tedious to be performed (especially for stiff problems) and in some cases may fail to converge during experimental data fitting. Here, an alternative procedure based on the derivation of a single differential equation is adopted. Differentiating equation (4)(b) with respect to time, we obtain:

$$
\begin{aligned}
\frac{d^2 P_v}{dt^2} = & -K_2 \left(\frac{dP}{dt} + \frac{dP_v}{dt} + \frac{dQ_x}{dt} + \frac{dD_e}{dt} + \frac{dP_{v_f}}{dt} \right) - K_3 \frac{dQ_x}{dt} \\
& -K_4 \frac{dD_e}{dt} - K_5 \frac{dP_{v_f}}{dt} \qquad (5)
\end{aligned}
$$

which, from (4), can be re-written as follows:

$$
\frac{d^2 P_v}{dt^2} + K_2 \frac{dP_v}{dt} + \tilde{K}^2 P_v = -K_2 \frac{dP}{dt} = K_1 K_2 AP \qquad (6)
$$

having assumed $\tilde{K}^2 = K_2(K_3 + K_4 + K_5) + K_3^2 + K_4^2 + K_5^2$.

Taking A moles equal to P moles, $\frac{dP}{dt}$ becomes:

$$
\frac{dP}{dt} = -K_1 P^2 \qquad (7)
$$

(7) is a first order differential equation with separable variables. Its integral is:

$$
P(t) = \frac{P_0}{(P_0 K_1 t + 1)} \qquad (8)
$$

Substituting (8) into (6) we obtain the following differential equation:

$$
\frac{d^2 P_v}{dt^2} + K_2 \frac{dP_v}{dt} + \tilde{K}^2 P_v = -K_2 \frac{dP}{dt} = \frac{K_1 K_2 P_0^2}{(P_0 K_1 t + 1)^2} \qquad (9)
$$

(9) is a non-homogeneous second order differential equation with constant coefficients.

From obvious physical considerations, it can be argued that $K_2 \gg K_3 \approx K_4 \approx K_5$ and hence $K_2/2 > \tilde{K}$, meaning that $(K_2/2)^2 - \tilde{K}^2 > 0$. Hence, the integral of the homogeneous part is trivial, i.e.:

$$P_v(t) = C_1 e^{(\alpha+\beta)t} + C_2 e^{(\alpha-\beta)t} \tag{10}$$

where C_1 and C_2 are two constants that can be determined from initial conditions, $\alpha = -1/2K_2$ and $\beta = \sqrt{(K_2/2)^2 - \tilde{K}^2}$.

The determination of the particular integral of (9) is not an easy task. In absence of consolidate ad-hoc procedures, the so-called general technique of the variation of the arbitrary constants should be used. However, such a general procedure provides only first derivatives of some functions entering in the particular integral and their analytical integration is in any case not possible. Here, an alternative procedure is proposed, which consists in substituting the original function, say $g(t)$, representing the right hand side of (9), with a fitting function in the following form:

$$f(t) = \gamma_1 e^{\gamma_2 K_1 P_o t} \tag{11}$$

where γ_1 and γ_2 are further constants to be determined in such a way that (11) fits as close as possible the non homogeneous term.

To make (11) near to the original function, we require that:

$$\begin{aligned} &f(0) = g(0) \\ &\int_0^{t_m \to \infty} f(t)dt = \int_0^{t_m \to \infty} g(t)dt \end{aligned} \tag{12}$$

Here it is worth noting that the first condition of (12) requires that functions f and g have the same initial value, whereas the second corresponds to impose that the average decay of unpolymerized reagent is the same, with the implicitly accepted simplifying hypothesis that at the end of the test (in practice for an infinite time) the unpolymerized reagent is negligible.

From (12) it can be shown that $\gamma_1 = \gamma_2 = 1$.

With the substitution adopted, a particular integral $P_v^p(t)$ is:

$$P_v^p(t) = K_1 K_2 P_0^2 \left[(K_1 P_0)^2 - K_2 (K_1 P_0) + \tilde{K}^2 \right]^{-1} e^{-K_1 P_0 t} \tag{13}$$

To fully solve the problem, it is necessary to determine constants C_1 and C_2. They are found from the following initial conditions as:

$$\begin{aligned} &P_v(0) = 0 \\ &\left.\frac{dP_v}{dt}\right|_{t=0} = K_2 P^*(0) = 0 \end{aligned} \tag{14}$$

After trivial algebra, it can be concluded that:

$$\begin{cases} C_2 = \rho\left(-\frac{K_1 P_0}{2\beta} - \frac{\alpha}{2\beta} - \frac{1}{2}\right) \\ C_1 = \rho\left(\frac{K_1 P_0}{2\beta} + \frac{\alpha}{2\beta} - \frac{1}{2}\right) \end{cases} \tag{15}$$

having defined $\rho = K_1 K_2 P_0^2 \left[(K_1 P_0)^2 - K_2 (K_1 P_0) + \tilde{K}^2\right]^{-1}$.

To summarize, the concentration of vulcanized polymer, during vulcanization, within the mixture obeys the following equation:

$$P_v(t) = C_1 e^{(\alpha+\beta)t} + C_2 e^{(\alpha-\beta)t} + \rho e^{-K_1 P_0 t}$$

$$\begin{cases} C_2 = \rho\left(-\frac{K_1 P_0}{2\beta} - \frac{\alpha}{2\beta} - \frac{1}{2}\right) \\ C_1 = \rho\left(\frac{K_1 P_0}{2\beta} + \frac{\alpha}{2\beta} - \frac{1}{2}\right) \\ \rho = K_1 K_2 P_0^2 \left[(K_1 P_0)^2 - K_2 (K_1 P_0) + \tilde{K}^2\right]^{-1} \\ \alpha = -\frac{K_2}{2} \\ \beta = \sqrt{(K_2/2)^2 - \tilde{K}^2} \\ \tilde{K}^2 = \tilde{K}^2 = K_2 (K_3 + K_4 + K_5) + K_3^2 + K_4^2 + K_5^2 \end{cases} \tag{16}$$

Kinetic constants to determine are only three, namely K_1, K_2 and $\tilde{K}^2$.

The most straightforward method to numerically estimate such kinetic constants is that followed in [34], relying into a experimental cure-curve data fitting, performed normalizing experimental data at peak to P_0 and translating the initial rotation resistance to zero, as suggested by Ding and Leonov [21].

In [34], K_1, K_2 and $\tilde{K}^2$ variables are found through a standard nonlinear least square routine. Here an alternative and more efficient model is utilized, which requires only 3 experimental data and allows a direct evaluation of the constants by means of the roots evaluation of three single variable non linear functions.

Furthermore, it is worth noting that K_1, K_2 and $\tilde{K}^2$ are temperature dependent constants. Therefore, also their variability with respect to absolute temperature should be investigated experimentally.

The simplest literature equation linking reaction constants to absolute temperature T is the so called Arrhenius law, which mathematically may be written as:

$$K_i(T) = K_{iA} e^{-K_{iB} T} \tag{17}$$

where K_{iA} and K_{iB} are two temperature independent constants.

From a mathematical point of view, from (16) and (17), it can be deduced that a total of 6 temperature independent reaction constants has to be identified numerically: K_{1A}, K_{1B}, K_{2A}, K_{2B}, $\tilde{K}_A$, $\tilde{K}_B$. As a consequence, at least 2 rheometer curves at two different absolute temperatures are needed to identify all constants. From a practical point of view, since in the $T - \log K_i(T)$ plane the Arrhenius law (17) is represented by a straight line, at least 3 experimental data at different temperatures are needed,

to deduce accurate values for K_{iA} and K_{iB} constants through a standard least square fitting procedure.

In Milani and Milani [34] experimental rheometer curves are represented, probably for the first time, assuming as vertical axis values normalized as $(M - M_m)/(M_{max} - M_m)$ and as horizontal axis the quantity $\log(t/t_{max})$, namely the logarithm of the normalized vulcanization time. This latter representation is practically very useful because it suggests to approximate both the experimental and numerical data provided by Eq. (16) by means of three straight lines. The slope of the last line well approximates reversion. Authors experienced that such a behavior is systematic, i.e. it occurs at any temperature for any compound and helps for a very practical characterization of reaction constants, as it will be shown hereafter.

At a fixed vulcanization temperature, by means of Eq. (16) and the chain rule, the first derivative of cross-linked polymer concentration with respect to $\log(t/t_{max})$ is:

$$\frac{dP_v(t)}{d\ln\frac{t}{t_{max}}} = t_{max}\frac{dP_v(t)}{d\ln t} = t_{max}t\frac{dP_v(t)}{dt}$$
$$\Rightarrow \frac{dP_v(t)}{d\ln\frac{t}{t_{max}}} = t_{max}t\left(C_1(\alpha+\beta)e^{(\alpha+\beta)t} + C_2(\alpha-\beta)e^{(\alpha-\beta)t} - \rho\tilde{K}_1 e^{-\tilde{K}_1 t}\right) \tag{18}$$

Having indicated with $\tilde{K}_1$ the quantity K_1P_0.

Observing that $\tilde{K}$ is small when compared with K_1 and K_2 it can be argued that for practical purposes $|\alpha| \approx |\beta| \approx K_2/2$, $\rho = P_0\tilde{K}_1K_2\left[\tilde{K}_1^2 - K_2\tilde{K}_1\right]^{-1} = P_0K_2/\left(\tilde{K}_1 - K_2\right)$. Therefore Eq. (18) can be re-written as:

$$\frac{dP_v(t)}{d\ln\frac{t}{t_{max}}} \approx t_{max}t\left(C_2(\alpha-\beta)e^{(\alpha-\beta)t} - \rho\tilde{K}_1e^{-\tilde{K}_1t}\right)$$
$$= t_{max}t\rho\tilde{K}_1\left(e^{-K_2t} - e^{-\tilde{K}_1t}\right) = P_0t_{max}t\frac{\tilde{K}_1K_2}{\tilde{K}_1 - K_2}\left(e^{-K_2t} - e^{-\tilde{K}_1t}\right) \tag{19}$$

Having at disposal the quantity $\frac{dP_v(t)}{d\ln\frac{t}{t_{max}}}$ in the $P_v(t) - \ln\frac{t}{t_{max}}$ plane at $t = t_0$ (first straight line), it is possible to find reaction kinetic constant $\tilde{K}_1$ graphically or by means of the numerical evaluation of the root of a single variable non linear equation as follows. Assuming that $K_2 \gg \tilde{K}_1$ (analogous considerations may be drawn in the case $\tilde{K}_1 \gg K_2$ (19) may be further simplified as follows, being $\tilde{K}_1 - K_2 \approx K_2$ and $e^{-K_2t_0} \approx 0$:

$$\left.\frac{dP_v(t)}{d\ln\frac{t}{t_{max}}}\right|_{t=t_0} \approx -P_0t_{max}t_0\tilde{K}_1e^{-\tilde{K}_1t_0} \tag{20}$$

Equation (20) root may be graphically determined finding the point of intersection of the following hyperbola y_1 and exponential function y_2:

$$y_1 = \left.\frac{\frac{dP_v(t)}{d\ln\frac{t}{t_{\max}}}}{P_0 t_{\max} t_0 \tilde{K}_1}\right|_{t=t_0}$$
$$y_2 = e^{-\tilde{K}_1 t_0} \tag{21}$$

In the case $K_2 \gg \tilde{K}_1$ a similar relation is derived. If a Newton-Raphson routine is at disposal, the graphical representation (21) can be avoided and the root can be found directly from (20).

To find K_2 we take again in consideration the Eq. (16). Assuming again $|\alpha| \approx |\beta| \approx K_2/2$ and $\rho = P_0 K_2 / \left(\tilde{K}_1 - K_2\right)$ Eq. (16) becomes:

$$\begin{aligned} P_v(t) &= C_1 - \rho\frac{\tilde{K}_1}{K_2}e^{-K_2 t} + \rho e^{-\tilde{K}_1 t} = \rho\left(\frac{\tilde{K}_1}{2\beta} - 1\right) - \rho\frac{\tilde{K}_1}{K_2}e^{-K_2 t} + \rho e^{-\tilde{K}_1 t} \\ &= \frac{P_0 K_2}{\left(\tilde{K}_1 - K_2\right)}\left(\frac{\tilde{K}_1}{K_2} - 1 + e^{-\tilde{K}_1 t} - \frac{\tilde{K}_1}{K_2}e^{-K_2 t}\right) \\ \Rightarrow P_v(t) &= P_0\left[1 + \frac{K_2}{\left(\tilde{K}_1 - K_2\right)}e^{-\tilde{K}_1 t} - \frac{\tilde{K}_1}{\left(\tilde{K}_1 - K_2\right)}e^{-K_2 t}\right] \end{aligned} \tag{22}$$

Once $\tilde{K}_1$ is known, (22) allows estimating K_2 by means of the procedure summarized in Table 1.

The first step consists in evaluating $N_{\exp}$ trial values of constant K_2, where $N_{\exp}$ is the number of sampled points (either experimental or deriving from another numerical model) where torque values are known. In the case $K_2 \gg \tilde{K}_1$ again $e^{-\tilde{K}_2 t} \approx 0$, with the obvious implication that (22) reduces to $P_v(t) = P_0\left(1 + \frac{K_2}{\tilde{K}_1 - K_2}e^{-\tilde{K}_1 t}\right)$. Assuming that $P_{\exp}(t_i)$ is the experimental normalized torque at t_i and assuming $P_v(t_i) = P_{\exp}(t_i)$, the direct evaluation of a trial value for K_2 at t_i is very straightforward:

Table 1 Pseudo-code of the function utilized for the simplified evaluation of K_2

$N_{\exp}$ experimental (or numerical) time values where torque is known

$\tilde{K}_1$, $P_{\exp}(t_i)$, t_i : known

Evaluate $K_2^{Trial}(t_i)$: trial value of K_2 at t_i

For i from 1 to $N_{\exp}$

Evaluate the total relative error assuming $K_2 = K_2^{Trial}(t_i)$ as follows

$$e_{K_2(t_i)} = \sum_{i=1}^{N_{\exp}} \frac{\left|P_0\left[1 + \frac{K_2^{Trial}}{\left(\tilde{K}_1 - K_2^{Trial}\right)}e^{-\tilde{K}_1 t_i} - \frac{\tilde{K}_1}{\left(\tilde{K}_1 - K_2^{Trial}\right)}e^{-K_2^{Trial} t_i}\right] - P_{\exp}(t_i)\right|}{P_{\exp}(t_i)}$$

Endfor

Assume K_2 equal to $K_2^{Trial}(t_i)$ that minimizes the total relative error

$$K_2(t_i) = \frac{P_{\exp}(t_i) - P_0}{P_{\exp}(t_i) + P_0 e^{-\tilde{K}_1 t_i} - P_0} \tag{23}$$

For each trial value of $K_2(t_i)$, hereafter called K_2^{Trial}, the total cumulative percentage error obtained with the model proposed is then estimated by means of (22) as follows:

$$e_{K_2(t_i)} = \sum_{i=1}^{N_{\exp}} \frac{\left| P_0 \left[1 + \frac{K_2^{Trial}}{\left(\tilde{K}_1 - K_2^{Trial}\right)} e^{-\tilde{K}_1 t_i} - \frac{\tilde{K}_1}{\left(\tilde{K}_1 - K_2^{Trial}\right)} e^{-K_2^{Trial} t_i} \right] - P_{\exp}(t_i) \right|}{P_{\exp}(t_i)} \tag{24}$$

where $N_{\exp}$ is the total number of sampled points.

The optimal K_2 among K_2^{Trial} values is obviously selected as that minimizing error (24).

With final values of $\tilde{K}_1$ and K_2 so obtained, $\tilde{K}$ is finally estimated assuming the value of the tangent line known in the descending branch at t_3 in the $\ln \frac{t}{t_{\max}} - P_v(t)$ plane (Eq. 18). In particular, such value is again provided by the exponential model as:

$$\left.\frac{dP_v(t)}{d\ln\frac{t}{t_{\max}}}\right|_{t=t_3} = t_{\max} t_3 \left(C_1(\alpha+\beta) e^{(\alpha+\beta)t_3} + C_2(\alpha-\beta) e^{(\alpha-\beta)t_3} - \rho \tilde{K}_1 e^{-\tilde{K}_1 t} \right)$$

$$\rho = K_1 K_2 P_0^2 \left[(K_1 P_0)^2 - K_2 (K_1 P_0) + \tilde{K}^2 \right]^{-1} \tag{25}$$

$$\alpha = -\frac{K_2}{2}$$

$$\beta = \sqrt{(K_2/2)^2 - \tilde{K}^2}$$

A standard numerical routine to find zeros of a non linear function with one variable $(\tilde{K})$ may be used to obtain an estimation of the constant.

3 Numerical applications

In order to assess the reliability of the simplified direct model proposed in reproducing sulphur cured EPDM crosslinking degree, two experimental data sets available in the literature [12] are here re-considered. Experimental data available rely into cure curves performed at different temperature conditions. Typically, three different temperatures are considered, in order to have an insight into the variability of kinetic constants with respect to temperature.

To perform a numerical optimization of the kinetic model proposed, experimental cure values are normalized dividing each point of the curve by the maximum torque values, so that experimental data are always within the range 0–1.

3.1 First data set

Experimental data used to perform the first set of numerical simulations are available from [12] at three increasing temperatures, namely 160, 180 and 200 °C. Rheometer charts were obtained by mean of a Monsanto Oscillating Disc Rheometer ODR with an arc deflexion of 3°. The compound exhibits a medium-high level of insaturation and it is therefore quite indicated to check the predictivity of the model proposed in presence of remarkable reversion. The composition of the EPDM hereafter considered is schematically summarized in Table 2.

In Fig. 3, a comparison among cure curve provided by the present approach, alternative numerical models and experimental results is sketched for a temperature equal to 160 °C.

Figure 3a is a classic rheometer chart, similar to Fig. 2, but with vertical axis values normalized as $(M - M_m)/(M_{max} - M_m)$, with M_m and M_{max} representing minimum and maximum torque values respectively, whereas in the second sub-figure the quantity $\log(t/t_{max})$ is represented in the horizontal axis, i.e. the logarithm of the normalized vulcanization time. This latter representation, whilst non-standard, is practically very useful because it suggests to approximate both the experimental and numerical data provided by Eq. (16) by means of three straight lines. The slope of the last line well approximates reversion. Authors experienced that such a behavior is systematic, i.e. it occurs at any temperature for any compound and helps for a very practical characterization of reaction constants.

In Fig. 3a, squares represent the few points utilized to fit experimental data through the second order differential equation model (16), sketched in the figure by means of a dashed line.

The continuous thick blue curve is the full experimental curve obtained by ODR tests, whereas the continuous line with diamond symbols is the representation, in the normalized rheometer chart, of Eq. (22). As it is possible to notice, the agreement among all models is almost perfect, within all the time range inspected. Even Eq. (22), which is a theoretical model without reversion, fits very well experimental data. This is not surprising, because very little or no reversion is expected at low curing temperatures.

Little discrepancy is found for the three-line model in a very strict time range near a crosslinking equal to 0.9. Again this behavior was expected, because the so-called three-line approximation is conceived exclusively to have an estimate of meaningful first derivative values (in the modified rheometer chart) of the cure curve, to successively evaluate directly, by means of Eqs. (21, 24) and (25) $\tilde{K}_1$, K_2 and $\tilde{K}$ values, without the utilization of a non-linear least square approach.

Once $\tilde{K}_1$, K_2 and $\tilde{K}$ are at disposal by means of the three-line approach, Eq. (16) may be used directly to fit experimental data with the exponential model.

In Table 3, a comparison between kinetic constants provided by the exponential model and the simplified direct method is summarized. The agreement is very satisfactory, with percentage errors not exceeding 5 % in the most unfavourable case, a result which seems very satisfactory having in mind the practical application of the model proposed.

Table 2 First and second data set rubber composition

Polymer type used	DUTRAL 4334	
% of Propylene content by wt	27	
% ENB by wt.	4.7	
% oil by wt.	30	
ML(1 + 4)125 °C	28	
First data set		
Formulation for white items	Description	in phr
Polymer	Dutral 4334	140
Zinc Oxide	Activator	5
Stearic acid	Co-agent	3
Clay	Filler	400
Titanium Bioxide	Co-agent whitener	15
Paraffinic oil	wax additive	40
Sulphur	vulcanization agent	2
TMTD Tetramethylthiuram disulfide	Accelerator	2
MBT2 Mercaptobenzothiazole	Acceleretor	2
Characteristics of the compound		
ML(1 + 4)100 °C	67	
ODR at 180 °C	t_2 1′06″	
	t_{90} 5′30″	
Characteristics of the vulcanized compound		
Tensile strength Kg/cm^2	80	
Elongation at break %	600	
Hardness Shore A	74	
Second data set		
Compound for black items	Description	in phr
Polymer	Dutral 4334	140
Zinc Oxide	Activator	5
Stearic acid	Co-agent	1
HAFN 330	Carbon black–filler	140
Paraffinic oil (Cortis 100M)	Wax additive	30
Sulphur	Vulcanization agent	1.5
TMTD Tetramethylthiuram disulfide	Accelerator	1.0
MBT2 Mercaptobenzothiazole	Acceleretor	0.5
Characteristics of the compound		
ML(1 + 4)100 °C	88	
ODR 200 °C	t_2 55″	
	t_{90} 1′54″	
Characteristics of the vulcanized compound		
Tensile strength Kg/cm^2	165	
Elongation at break %	310	
Hardness shore A	73	

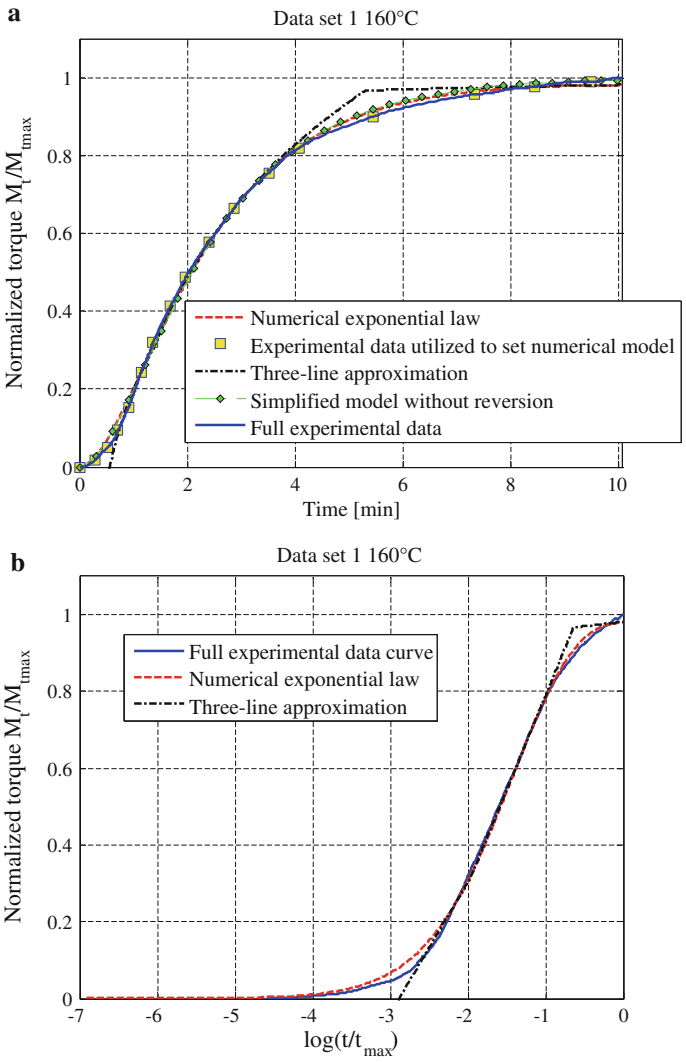

Fig. 3 First data set at 160 °C. **a** Traditional rheometer charts. **b** Rheometer charts in normalized logarithmic scale

Comparisons among all models for temperatures equal to 180 and 200 °C are replicated in Figs. 4 and 5 respectively, again with a twofold graphical representation. Also in these latter cases, the agreement with the experimental response seems quite accurate. As can be noted, very few experimental points are needed to obtain a rather satisfactory reproduction of the actual experimental curve.

As expected, reversion is rather marked at 200 °C, but has a perceivable effect also for the curing curve at 180 °C. As expected, in both these latter cases, Eq. (22) model progressively loses is accuracy, especially at increasing curing times, being reversion completely disregarded in the model.

Table 3 First data set

Kinetic constant (1/sec)	Exponential model non linear least squares	Present direct model	Percentage error (%)
160 °C			
K_1	0.5671	0.5718	−0.83
K_2	1.2567	1.2418	1.18
$\tilde{K}$	0.0492	0.0477	3.05
180 °C			
K_1	0.8903	0.9101	−2.22
K_2	2.5501	2.4374	4.42
$\tilde{K}$	0.1610	0.1578	1.99
200 °C			
K_1	1.8106	1.7469	3.52
K_2	7.5407	7.9126	−4.93
$\tilde{K}$	0.5702	0.5839	−2.40

Comparison between kinetic constants evaluated by means of the exponential model and the simplified direct model

For the sake of completeness in Fig. 6 hyperbolae y_1 and exponential functions y_2 defined in Eq. (21) for the graphical determination of constant $\tilde{K}_1$ (as intersection point between y_1 and y_2), are represented for the three temperatures inspected. As it is possible to notice, the graphical determination of constant $\tilde{K}_1$ at different temperatures is very straightforward and may be obtained without any effort.

Having at disposal, from the numerical model, all the three kinetic constants at three different temperatures, it is possible to check if such kinetic constants follow an Arrhenius law with respect to temperature. At this aim, numerical values are plotted in the Arrhenius space (1/T–log(Ki) plane), to see if they lay on a straight line. Figure 7 shows, for the three kinetic constants under consideration, the linear regression obtained in the Arrhenius space (squares, circles and triangles represent kinetic constants found with the single differential equation model, fitting experimental data). As it is possible to notice, all the three K_i seem to follow roughly an Arrhenius law of the type $K_i = K_{i0}e^{-E_{ai}/RT}$, having defined with $\log K_{i0}$ the y-value of the regression lines in the Arrhenius space for 1/T equal to zero (i.e. kinetic constant at infinite temperature) and E_{ai} the reaction activation energy, being R the gas constant.

With reference to Fig. 7, where a comparison between the three kinetic constants provided by the model are reported, the following considerations may be deduced:

1. As expected, values found for K_1 and K_2 are higher than values for $\tilde{K}$, which is the combination of final vulcanization and devulcanization in all experimental range and for EPDM with low and high insaturation. While reversion is present at high temperatures for both compounds, obviously devulcanization is a phenomenon that interests a relatively small amount of crosslinked polymer. Devulcanization sensibly increases with temperature, as correctly predicted by the model (increase of constant $\tilde{K}$). As expected, devulcanization is quite critical, the blend under

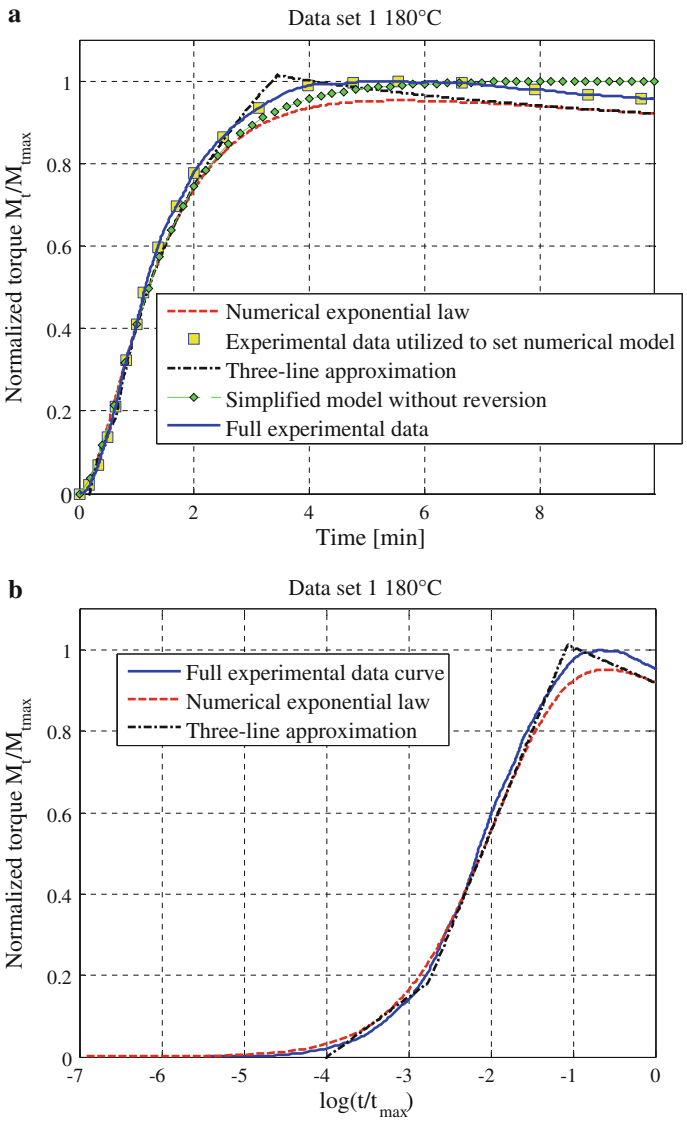

Fig. 4 First data set at 180 °C. **a** Traditional rheometer charts. **b** Rheometer charts in normalized logarithmic scale

consideration exhibiting relatively big values of $\tilde{K}$ (comparable with K_1 values) at high vulcanization temperatures.

2. The observation that K_1 values are, in any case, systematically higher than $\tilde{K}$ values and generally lower than K_2, may be justified by the fact that the reaction between the polymer and accelerator is very fast and sensible to temperature variation. Therefore, it is crucial to homogenize the compounds, during the mixing of polymers, filler, accelerators, sulfur and other additives and co-adjuvants.

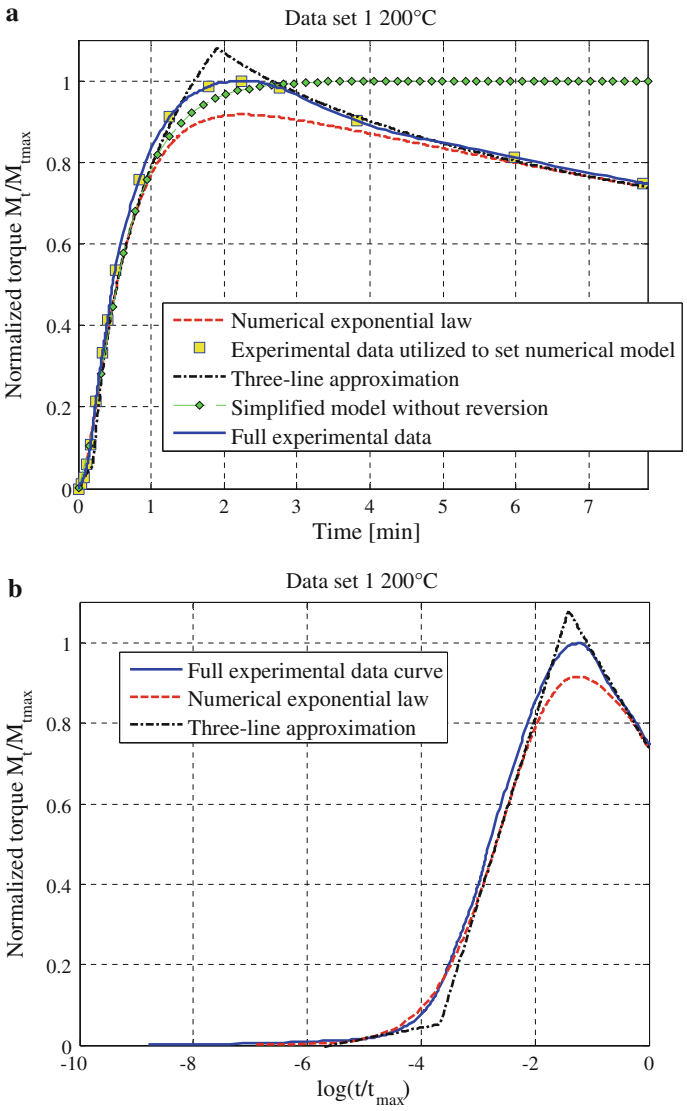

Fig. 5 First data set at 200 °C. **a** Traditional rheometer charts. **b** Rheometer charts in normalized logarithmic scale

3. K_2 values are systematically higher than K_1 and this justifies the strong mathematical hypothesis to assume $K_2 \gg K_1$. This means that the formation of the initial cross-linking is not influenced by small and big amount of ENB.
4. $\tilde{K}$ values increase considerably at high temperatures. Ideally, a temperature where the value of $\tilde{K}$ equates the value of K_1 may be easily found intersecting corresponding regression lines in the Arrhenius plane. In this case, the intersection point corresponds roughly to a temperature equal to 240 °C. Such a value may be considered as the limit over vulcanization of any item constituted by the compound

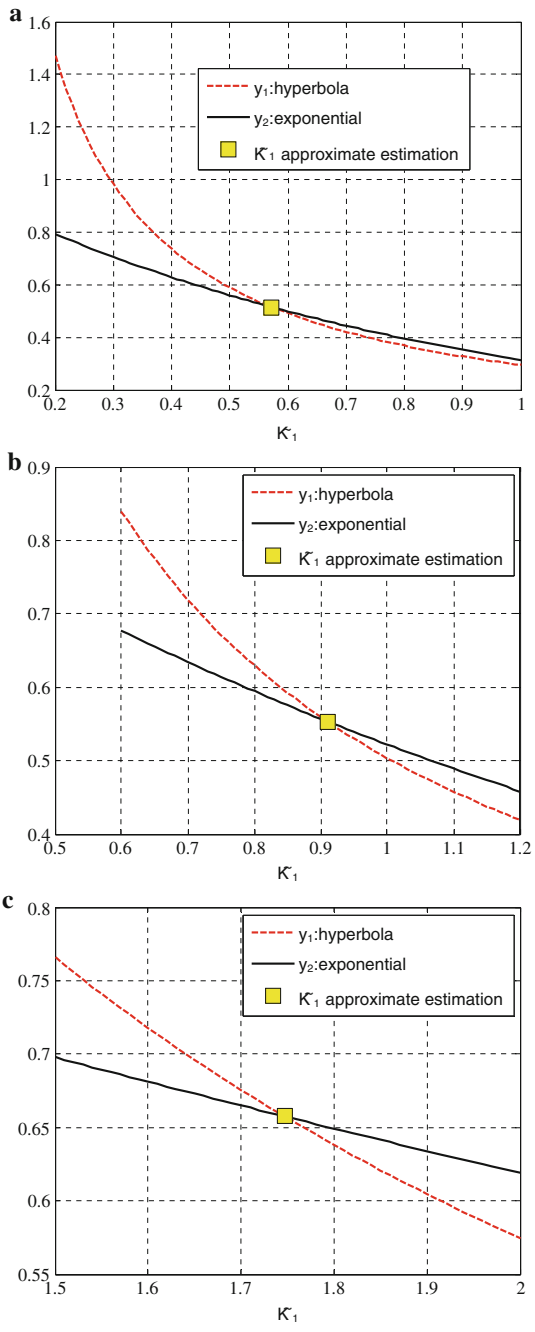

Fig. 6 First data set. Graphical determination of constant $\tilde{K}_1$ basing on Eq. (21). **a** 160 °C. **b** 180°C. **c** 200 °C

under consideration is theoretically impossible, being there the rate of vulcanization equal to the rate of devulcanization. In practice, very inefficient curing occurs even at lower temperatures, say 220−210 °C.

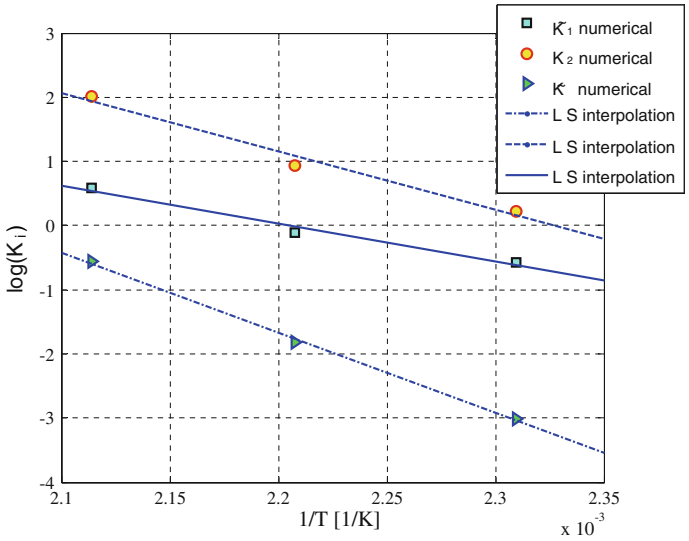

Fig. 7 First data set. Linear regression interpolation of the kinetic constants provided by the single differential equation model in the Arrhenius space (1/T–log(K_i))

3.2 Second data set

The second set of experimental data available [12] refers to an EPDM compound with little unsaturations, where reversion at high temperature is relatively small. Experimental cure curves available were collected at three increasing temperatures, namely 160, 180 and 200 °C. The exact composition of the blend analyzed is summarized in Table 2.

In Fig. 8, a comparison among rheometer curve obtained with the present model, exponential model (16), experimental data and model without reversion (Eq. 22) is depicted. Excellent agreement with all results is found. Reversion is in practice null, as confirmed both by the small values of constant $\tilde{K}$ reported in Table 4 and by the three-line approximation represented in Fig. 8b. As it is possible to notice, indeed, the third approximating line is almost horizontal, meaning that its slope (directly connected to $\tilde{K}$ value) is almost zero. The practical utility of the non-standard rheometer chart represented in Fig. 8b is very straightforward in this case, suggesting a direct rough estimation of the actual values of kinetic constants involved in the vulcanization process.

Comparisons among all models are replicated in Figs. 9 and 10 for vulcanization temperatures equal to 180 and 200 °C respectively. Again, the agreement among all different models is very satisfactory. Reversion is in this case very small, with a slight increase for external vulcanization temperature equal to 200 °C. Being in this case reversion less critical, the simplified model provided by Eq. (22) is capable of providing relatively good results even at high temperatures.

Analogously to what done in the previous case, for the sake of completeness, in Fig. 11 hyperbolae y_1 and exponential functions y_2 defined in Eq. (21) are represented for the three temperatures inspected, in order to determine graphically constant $\tilde{K}_1$ as intersection point between y_1 and y_2.

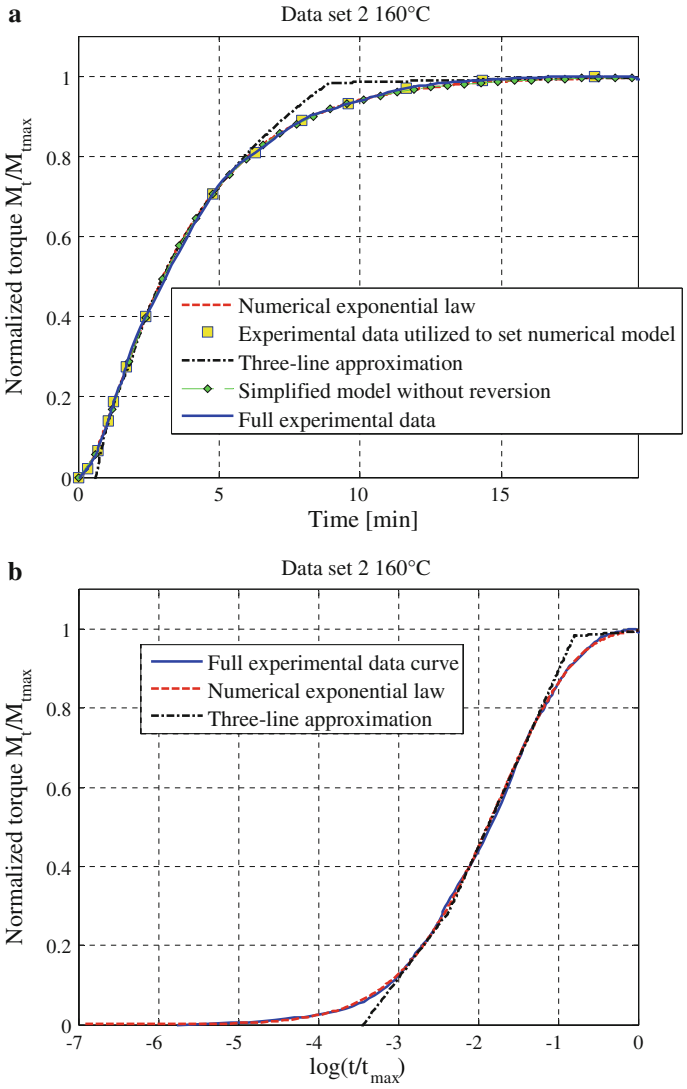

Fig. 8 Second data set at 160 °C. **a** Traditional rheometer charts. **b** Rheometer charts in normalized logarithmic scale

In Table 4, a full comparison between kinetic constants provided by the exponential model and the simplified direct method here proposed for the second data set is summarized. The agreement is almost perfect for all the temperatures inspected, with a percentage error in practice negligible for practical purposes.

Again, having at disposal from the numerical model the three kinetic constants at three different temperatures, it is possible to check if they follow an Arrhenius law, simply plotting numerical results in the Arrhenius space (1/T–log(Ki) plane). Figure 12 shows that a linear regression for K_1, K_2 and $\tilde{K}$ seems quite adequate with small deviation of the sampled values from the regression line. This result confirms again that

Table 4 Second data set

Kinetic constant (1/sec)	Exponential model non linear least squares	Present direct model	Percentage error (%)
160 °C			
K_1	0.3054	0.3000	1.77
K_2	1.4612	1.5074	−3.16
$\tilde{K}$	0.00791	0.00803	−1.52
180 °C			
K_1	0.5941	0.5950	−0.15
K_2	2.5303	2.5226	0.30
$\tilde{K}$	0.0201	0.0202	−0.49
200 °C			
K_1	1.7512	1.7679	−0.95
K_2	5.4486	5.3588	1.65
$\tilde{K}$	0.2247	0.2228	0.85

Comparison between kinetic constants evaluated by means of the exponential model and the simplified direct model

partial kinetic constants seem to obey an Arrhenius law of the type $K_i = K_{i0}e^{-E_{ai}/RT}$, with meaning of the symbols already discussed for the previous example.

Having an insight into Fig. 12, it is possible to do the following considerations:

1. As expected, again values found for K_1 and K_2 are higher than values for $\tilde{K}$, which synthetically represents oxidation, desulphuration and devulcanization reactions. This behavior is systematic and may be appreciated in all experimental range inspected. While reversion is present at high temperatures also in this case, here it is much less marked, thanks to the small amount of insaturations within the blend. From a mathematical point of view, this issue may be immediately checked comparing the slope of the regression line relevant for $\tilde{K}$ corresponding to the two cases analyzed, see Figs. 7 and 12.
2. Devulcanization seems to have perceivable effects in the rheometer chart only for temperatures exceeding 200 °C. This behavior is again correctly predicted by the model (increase of constant $\tilde{K}$ at high temperatures in Fig. 12 and decrease of the numerical rheometer curve at 200 °C in Fig. 10). However, values found for $\tilde{K}$ remain relatively small even at high temperature and in any case sensibly lower than values of constants K_1 and K_2 (respectively around 1/9 and 1/25). This remark again confirms that, as correctly predicted by the model, devulcanization is here less critical, with very small reversion (in practice negligible) for temperatures lower than 180 °C.
3. K_2 values are generally higher than K_1. Differently to the previous case, the slope of the regression lines for K_1 and K_2 is quite similar and an inversion of such a behavior is not expected in the range of temperatures where curing is practically possible. From a physical point of view, it can be stated that the formation of pendent sulphur (reaction associated to K_1) and crosslink (associated to K_2) always proceed with the same velocity rate.

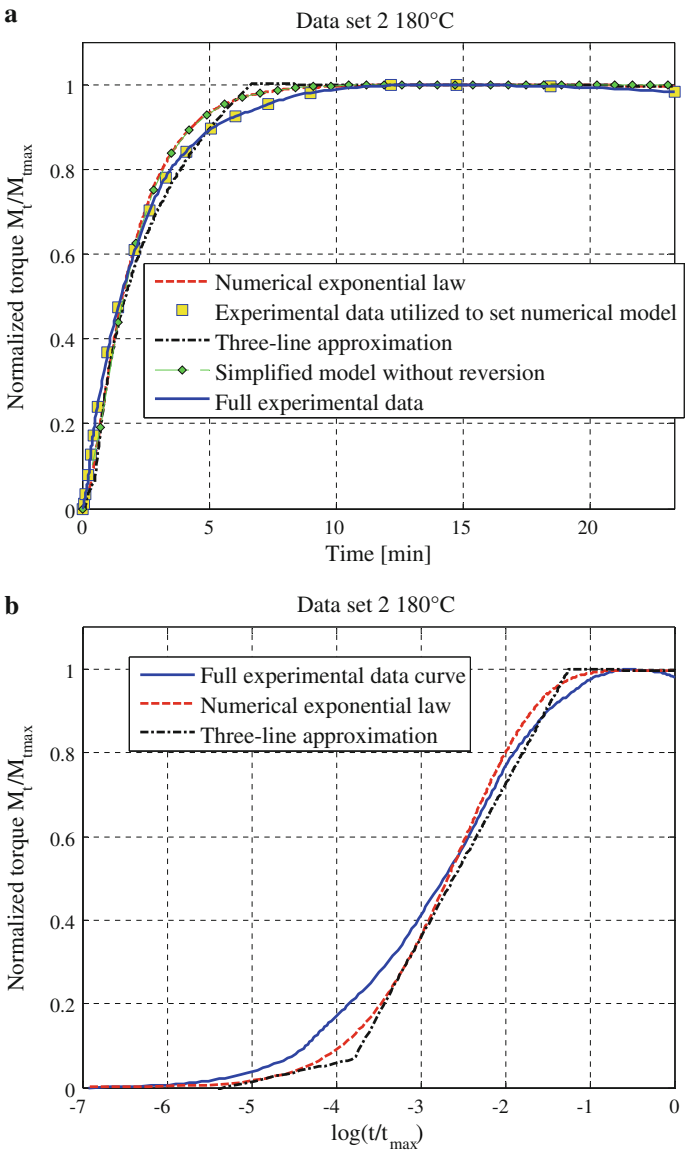

Fig. 9 Second data set at 180 °C. **a** Traditional rheometer charts. **b** Rheometer charts in normalized logarithmic scale

4. Extrapolating regression lines data, it can be seen that line representing $\tilde{K}$ does not cross either K_1 or K_2 regression lines, meaning that a blend with very small amount of insaturations is very stable, even at very high temperatures. This implies that, at least from a theoretical point of view, a good vulcanization level may be achieved at very high temperatures and quite reduced curing times, with a clear economical advantage for the producers.

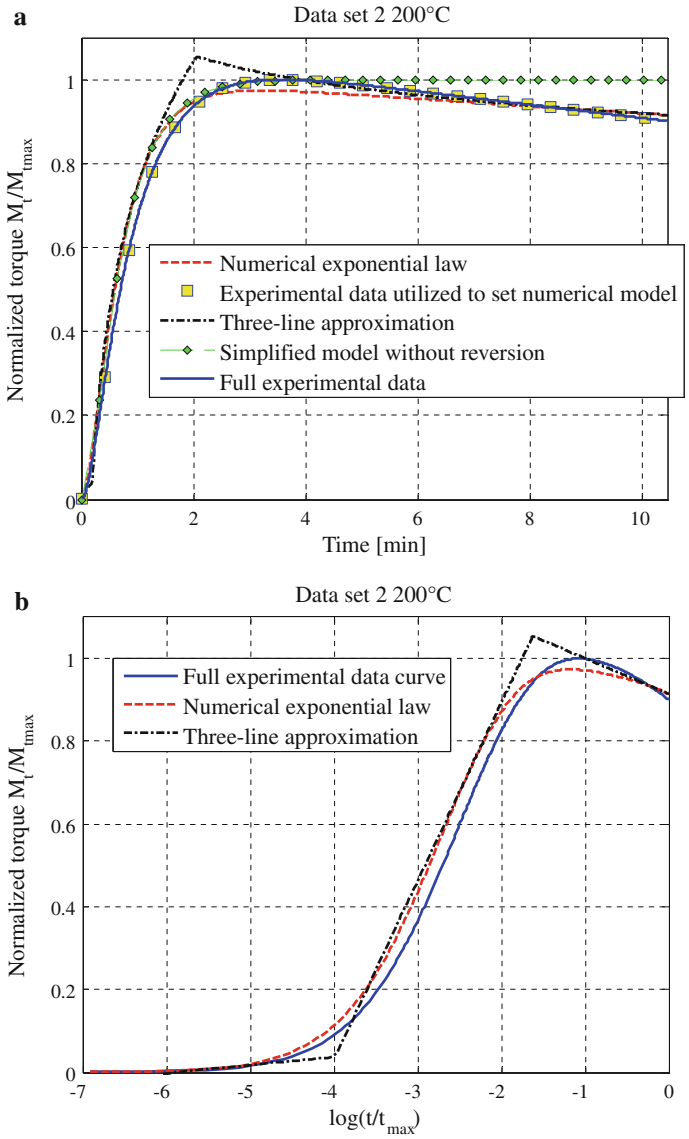

Fig. 10 Second data set at 200 °C. **a** Traditional rheometer charts. **b** Rheometer charts in normalized logarithmic scale

4 Conclusions

In the present paper, a direct method to determine reaction kinetic constants within an existing mathematical procedure [32] interpreting EPDM accelerated sulphur curing has been presented.

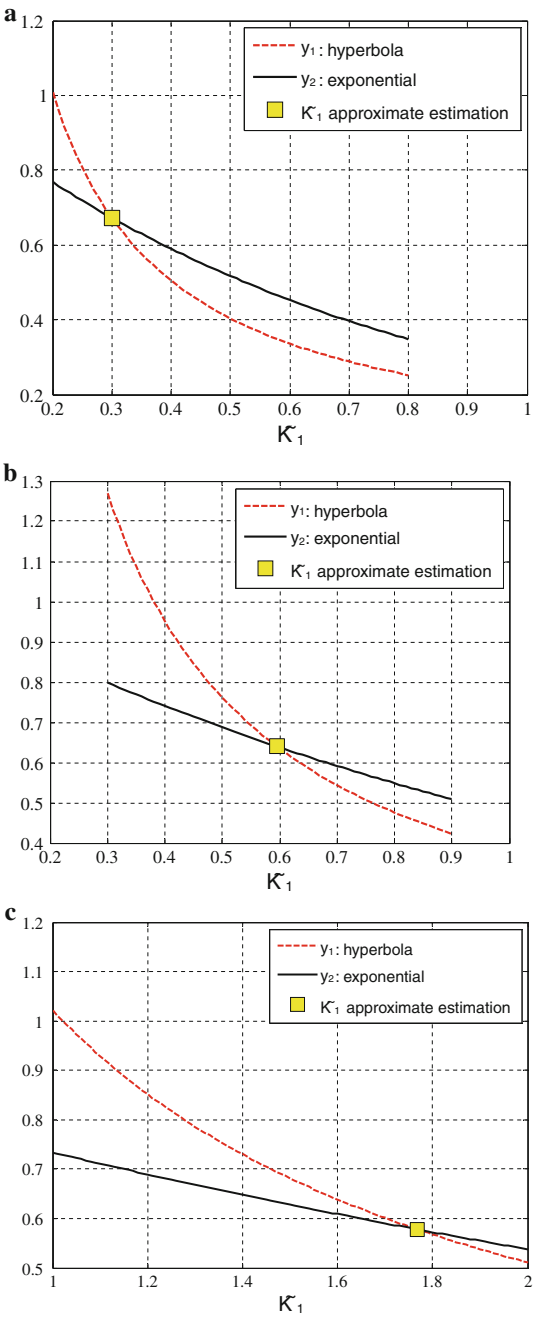

Fig. 11 Second data set. Graphical determination of constant $\tilde{K}_1$ basing on Eq. (21). **a** 160 °C. **b** 180 °C. **c** 200 °C

The model bases on a preliminary characterization of rubber through standard rheometer tests and allows an accurate prediction of the crosslinking degree at both successive curing times and different controlled temperatures.

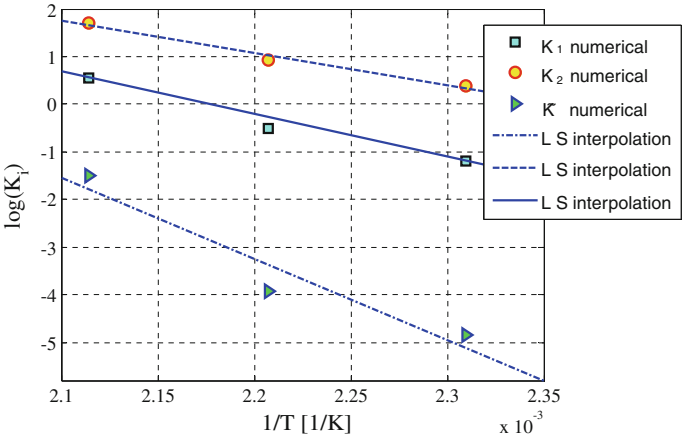

Fig. 12 Second data set. Linear regression interpolation of the kinetic constants provided by the single differential equation model in the Arrhenius space (1/T–log(K_i))

While in [32] a calibration of three kinetic constants at fixed temperature by means of non-linear least square fitting was required, here a simple model based on closed form formulas, derived from meaningful simplifications of the original rigorous approach has been utilized.

The applicability of the procedure is immediate and makes the model extremely appealing when fast and reliable estimates of crosslinking density of cured EPDM are required.

The evaluation of kinetic constants bases on the knowledge of rheometer charts, for the blend considered, at three or more vulcanization temperatures. Hence, rheometer test remains the key experimental device to study the kinetics of crosslinking for accelerated sulphur vulcanization.

As a matter of fact, from the basic mechanisms of accelerated sulphur vulcanization of EPDM and the experimental rheometer data, it is possible to directly determine K_1, K_2 and $\tilde{K}$ kinetic constants represented in Figs. 7 and 12.

Such constants represent physically the rates of partial reactions schematically shown in Fig. 1. Within the direct mathematical method proposed to solve the differential equation model (16), we can draw the following considerations:

1. All K_i partial kinetic constants seem to follow roughly an Arrhenius law. The analytical knowledge of K_i dependence on the temperature is extremely useful when it is necessary to evaluate the kinetic behavior of a blend for a temperature not coinciding with those selected for rheometer tests.
2. The variation of the reaction constant in the Arrhenius space is systematically big for $\tilde{K}$ and small for K_1, meaning that reversion is strongly dependent on vulcanization temperature.
3. From numerical simulations, it can be deduced that the utilization of EPDM with considerable amount of ENB content, results in an increase of the crosslinking precursor formation, a lower EPDM initial crosslinking, and a marked increase of the velocities of the three multiple reactions that can be associated to reversion and devulcanization.

4. As a consequence of the above considerations, it is possible to deduce that, if the vulcanization temperature increases, there is a decrease of the time necessary to reticulation, but an increase of reversion and probably a decrease of the mechanical properties of the items (in particular the stress-strain curve associated to the final vulcanized item will exhibit a less stiff behavior). All these considerations are quite important for manufactures interested in improving cured rubber mechanical properties, in changing vulcanization temperature, time, recipes and polymer types. Finally, the maximization of rubber performances at the same time reducing production costs as a function of the vulcanization technology adopted, is another issue that can be tackled with the approach prosed.

References

1. J.A. Brydson, *Rubbery Materials and Their Compouds* (Elsevier publisher Ltd, Exxex, 1988)
2. C. Goodyear, US Patent 3633 (1844)
3. F.W. Billmeier Jr, *Textbook of Polymer Science*, 3rd edn. (Wiley, London, 1984)
4. M. Morton (ed.), *Rubber Technology*, 2nd edn. (Van Nostrand Reinhold, New York, 1981)
5. L. Bateman (ed.), *The Chemistry and Physics of Rubber-Like Substances* (MacLaren, London, 1963)
6. M.L. Krejsa, J.L. Koenig, Solid state CNMR studies of vulcanized elastomers. XI. N-t-Butyl benzothiazole sulfenimide accelerated sulphur vulcanization of cis-polyisoprene at 75 MHz. Rubber Chem. Technol. **66**, 73–82 (1993)
7. M.L. Krejsa, J.L. Koenig, A review of sulphur cross-linking fundamentals for accelerated and unaccelerated vulcanization. Rubber Chem. Technol. **66**, 376–410 (1993)
8. C.H. Chen, E.A. Collins, J.R. Shelton, J.L. Koenigs, Compounding variables influencing the reversion process in accelerated curing of natural rubber. Rubber Chem. Tech. **55**(4), 1221–1232 (1982)
9. C.T. Loo, High temperature vulcanization of elastomers: 2. Network structures in conventional sulphenamide-sulphur natural rubber vulcanizates. Polymer **15**(6), 357–365 (1974)
10. N.J. Morrison, M. Porter, in *Crosslinking of rubbers*, ed. by G. Allen The Synthesis, Characterization, Reactions and Applications Of polymers (Pergamon press, Oxford, 1984)
11. S.K. Henning, The use of coagents in sulfur vulcanization: functional Zinc Salts. in *Proceedings of Spring 167*th *Technical Meeting of the Rubber Division* (American Chemical Society, San Antonio, 2005)
12. L. Corbelli, S. Codiglia, S. Giovanardi, F. Milani, G.C. Ottavi, R. Zucchini, *36*th *Report Montedison to B.F.Goodrich* (1977)
13. B.T. Poh, K.W. Wong, Effect of blend ratio on Mooney scorch time of rubber blends. J. Appl. Polym. Sci. **69**, 1301–1305 (1998)
14. B.T. Poh, C.C. Ng, Effect of silane coupling agents on the Mooney scorch time of silica-filled natural rubber compound. Eur. Polym. J. **34**, 975–979 (1998)
15. B.T. Poh, M.F. Chen, B.S. Ding, Cure characteristics of unaccelerated sulfur vulcanization of epoxidized natural rubber. J. Appl. Polym. Sci. **60**, 1569–1574 (1996)
16. B.T. Poh, C.S. Te, Dependence of Mooney scorch time of SMR L, ENR 25, and ENR 50 on concentration and types of antioxidants. J. Appl. Polym. Sci. **74**, 2940–2946 (1999)
17. B.T. Poh, E.K. Tan, Mooney scorch time and cure index of epoxidized natural rubber in presence of sodium carbonate. J. Appli. Polym. Sci. **82**, 1352–1355 (2001)
18. B.T. Poh, H. Ismail, K.S. Tan, Effect of filler loading on tensile and tear properties of SMR L/ENR 25 and SMR L / SBR blends cured via a semi-efficient vulcanization system. Polym. Test. **21**, 801–806 (2002)
19. ASTM D 5289-07 and ASTM D 2084-81. Annual Book of ASTM Standards, 2007 & 1986
20. J.S. Dick, H. Pawlowski, Alternate instrumental methods of measuring scorch and cure characteristics. Polym. Test. **14**, 45–84 (1995)
21. R. Ding, I. Leonov, A kinetic model for sulfur accelerated vulcanization of a natural rubber compound. J. Appl. Polym. Sci. **61**, 455–463 (1996)
22. R. Ding, I. Leonov, A.Y. Coran, Study of the vulcanization kinetics of an accelerated-sulfur SBR compound. Rubber Chem. Technol. **69**, 81 (1996)

23. V. Duchacek, M. Duskova, Cure curve with two plateaus—the result of individual vulcanization reactions. J. Polym. Eng. **21**, 341 (2001)
24. M.R. Kamal, S. Sourour, Kinetics and thermal characterization of thermoset cure. Polym, Eng, Sci. **13**, 59 (1973)
25. A. Arrillaga, A.M. Zaldua, R.M. Atxurra, A.S. Farid, Techniques used for determining cure kinetics of rubber compounds. Eur. Polym. J. **43**, 4783–4799 (2007)
26. A. De Falco, A.J. Marzocca, M.A. Corcuera, A. Eceiza, I. Mondragon, G.H. Rubiolo, S. Goyanes, Accelerator adsorption onto carbon nanotubes surface affects the vulcanization process of styrene–butadiene rubber composites. J. Appl. Polym. Sci. **113**, 2851–2857 (2009)
27. G. Natta, G. Crespi, G. Mazzanti, Ethylene-Propylene copolymers containing unsaturations. in *4*th *Rubber Technology Conference*, London, pp. 1–12 (1962)
28. G. Natta, G. Crespi, G. Mazzanti, Copolimeri etilene propilene contenenti insaturazioni. L'industria della gomma [In Italian, the rubber industry]. pp. 1–7 (1963)
29. A.Y. Coran, Vulcanization, in: *Science and Technology of Rubber*, chap. 7. (Academic Press, New York, 1978)
30. M. van Duin, Kaut. Gummi Kunststoffe, 55 Jarghang, 2 (2002)
31. G. Milani, F. Milani, A new simple numerical model based on experimental scorch curve data fitting for the interpretation of sulphur vulcanization. J. Math. Chem. **48**, 530–557 (2010)
32. G. Milani, F. Milani, A three function numerical model for the prediction of vulcanization-reversion of rubber during sulfur curing. J. Appl. Poly. Sci. **119**, 419–437 (2011)
33. G. Milani, F. Milani, EPDM accelerated sulfur vulcanization: a kinetic model based on a genetic algorithm. J. Math. Chem. **49**(7), 1357–1383 (2011)
34. G. Milani, F. Milani, Simple kinetic numerical model based on rheometer data for Ethylene–Propylene–Diene Monomer accelerated sulfur crosslinking. J. Appl. Polym. Sci. **124**(1), 311–324 (2012)
35. G. Padmavathia, M.G. Mandanb, S.P. Mitrab, K.K. Chaudhuri, Neural modelling of Mooney viscosity of polybutadiene rubber. Comput. Chem. Eng. **29**(7), 1677–1685 (2005)
36. G. Evans, J. Blackledge, P. Yardley, *Numerical Methods for Partial Differential Equations*, 2nd edn. (Springer, Berlin, 2001)
37. T.F. Coleman, Y. Li, Mathe. Program. **67**(2), 189–224 (1994)